

See discussions, stats, and author profiles for this publication at: <https://www.researchgate.net/publication/231409222>

Regular and irregular spatial patterns in an immobilized-catalyst Belousov-Zhabotinsky reaction

ARTICLE *in* THE JOURNAL OF PHYSICAL CHEMISTRY · APRIL 1989

Impact Factor: 2.78 · DOI: 10.1021/j100344a016

CITATIONS

52

READS

22

3 AUTHORS, INCLUDING:



[Jerzy Maselko](#)

University of Alaska Anchorage

44 PUBLICATIONS 667 CITATIONS

[SEE PROFILE](#)



[Kenneth Showalter](#)

West Virginia University

124 PUBLICATIONS 5,590 CITATIONS

[SEE PROFILE](#)

FKN mechanism of the BZ reaction (expanded "Oregonator") agree surprisingly well with the experimental data. Similar conclusions hold in the case when the system of two coupled CSTR's with forcing of one of them is investigated.³² Both permanent and temporal extinction of oscillations are observed and modeled.^{33,34}

Early experimental observations of complex chemical wave trains generated by periodic perturbations are due to Showalter, Noyes, and Turner.²² They used the BZ reaction on a Petri dish periodically perturbed by voltage pulses on a Pt-Ag electrode couple. Farey ordering of periodic wave trains and a devil's-staircase-like structure in a similar experimental system were reported in ref 25. We consider the narrow tube used here to be a more controllable experimental system than the Petri dish. It is satisfactory that the results of the experiments reported here

agree well with those published previously.²⁵ When periodically forced, both oscillatory and excitable BZ systems reveal striking similarities in the arrangement of resonance regions and in parameter dependences of the firing number. Despite the lack of any apparent periodicity in the unperturbed excitable system, a "latent" periodicity is excited by the forcing. The difference between such a "latent" periodicity and a true one is reflected in the fact that the firing number ranges only from 0 to 1 in the forced excitable system while it may take on an arbitrary value in the forced oscillatory system. There seems to exist already a solid basis of experimental studies on periodic perturbations of chemical oscillations; cf. papers by Rehms and Ross in ref 2 and the paper by Schneider³⁵ for a review. We believe that a similar basis should be built for chemical excitable systems.

Registry No. BrO₃⁻, 15541-45-4; malonic acid, 141-82-2; ferroin, 14708-99-7.

(33) Dolník, M.; Marek, M. *J. Phys. Chem.* 1988, 92, 2452.

(34) Crowley, M. F.; Epstein, I. R. *J. Phys. Chem.*, in press.

(35) Schneider, F. V. *Annu. Rev. Phys. Chem.* 1985, 36, 347.

Regular and Irregular Spatial Patterns in an Immobilized-Catalyst Belousov-Zhabotinsky Reaction

Jerzy Maselko,[†] John S. Reckley, and Kenneth Showalter*

Department of Chemistry, West Virginia University, Morgantown, West Virginia 26506-6045

(Received: July 29, 1988)

Unusual spatial patterns are exhibited in a Belousov-Zhabotinsky reaction in which the ferroin catalyst is immobilized on cation-exchange resin. A thin layer of ferroin-loaded resin beads covered with solution containing bromate, malonic acid, and sulfuric acid exhibits propagating chemical waves for periods in excess of 100 h. The number of spontaneous wave initiation sites increases with increasing concentration of sulfuric acid or bromate, and above a critical concentration only counterrotating spirals are initiated. An overcrowding of these sites at high sulfuric acid or bromate concentrations results in irregular patterns with features suggestive of phase turbulence.

Introduction

Luther¹⁻³ was apparently the first to recognize that the diffusive spread of an autocatalyst in a chemically reacting mixture may give rise to propagating waves of accelerated reaction. Most studies of chemical waves since this early investigation have focused on initially homogeneous reaction mixtures.^{4,5} No investigations of condensed-phase reactions with immobilized catalysts have been reported, although this configuration is common in many chemical processes. A related configuration is found in surface-catalyzed gas-phase reactions, and pattern formation in oscillatory reactions such as the oxidation of H₂ on Pt foil and supported Pt has been investigated.⁶ We report here studies of spatial behavior in the Belousov-Zhabotinsky (BZ) reaction in which the ferroin catalyst is immobilized on cation-exchange resin.

Many factors make an immobilized-catalyst, oscillatory reaction attractive for study. A system in which reaction occurs only at the immobilized catalyst provides an experimental realization of the "pool-chemical" approximation,⁷ with reactants at almost constant concentrations supplied from a large reservoir. Large differences in the effective diffusion coefficients of the reacting species occur naturally in immobilized-catalyst systems, enhancing the possibility of stationary patterns⁸⁻¹¹ and spatial chaos.^{12,13} In addition, an open system is readily configured, offering better control of experimental constraints.

Several studies of BZ chemical waves in open reactors have been recently reported. Waves propagating unidirectionally in a ring reactor made of acrylamide gel have been investigated,

TABLE I: System Composition^a

[KBrO ₃] = 0.05-0.50 M
[H ₂ SO ₄] = 0.25 M
[CH ₂ (COOH) ₂] = 0.025 M
[ferroin] = 1.0 × 10 ⁻⁵ mol/g resin

^a 200.0 mL of solution mixed with 5.0 g of loaded resin.

TABLE II: Cation-Exchange Resin^a

size	mesh	bead diameter/ μm
1	>400	38-75
2	200-400	75-150
3	100-200	106-250
4	50-100	180-425
5	20-50	300-1180

^a Bio-Rad Analytical Grade 50W-X4.

where reactants are diffusively replenished from interior and exterior reservoirs.¹⁴ Progress has also been made in the sys-

- (1) Luther, R. *Elektrochem.* 1906, 12(32), 596.
- (2) Arnold, R.; Showalter, K.; Tyson, J. J. *J. Chem. Educ.* 1987, 64, 740.
- (3) Showalter, K.; Tyson, J. J. *J. Chem. Educ.* 1987, 64, 742.
- (4) Field, R. J.; Burger, M., Eds. *Oscillations and Traveling Waves in Chemical Systems*. Wiley: New York, 1984.
- (5) Winfree, A. T. *The Geometry of Biological Time*; Springer-Verlag: New York, 1980.
- (6) Schmitz, R. A.; D'Netto, G. A.; Razon, L. F.; Brown, J. R. In *Chemical Instabilities*; Nicolis, G., Baras, F., Eds.; Reidel: Boston, 1984; pp 33-57.
- (7) Gray, P.; Scott, S. K. *Bunsen-Ges. Phys. Chem.* 1986, 90, 985.
- (8) Prigogine, I.; Nicolis, G. *J. Chem. Phys.* 1967, 46, 3542.
- (9) Becker, P. K.; Field, R. J. *J. Phys. Chem.* 1985, 89, 118.

[†]On leave from the Institute of Inorganic Chemistry and Metallurgy of Rare Elements, Technical University, Wroclaw, Poland.

tematic variation of constraints by using a continuously fed unstirred reactor.¹⁵

In this paper we focus on the properties of an excitable medium that is "uniformly inhomogeneous". By varying either the reaction mixture composition or the mesh size of the cation-exchange resin, we are able to examine systems that range from effectively continuous to effectively discrete. Our studies show that the nature and density of randomly distributed wave initiation sites dramatically affect pattern formation. These features are of obvious importance in the excitable media of biological systems such as aggregates of cells or reactive sites on a membrane.

Experimental Section

Materials and Equipment. Stock solutions of KBrO_3 , $\text{CH}_2(\text{COOH})_2$, H_2SO_4 , and $\text{Fe}(\text{phen})_3\text{SO}_4$ were prepared with doubly distilled water and reagent grade chemicals. The concentrations of the malonic acid and sulfuric acid solutions were determined by titration with standard base. The concentrations of the potassium bromate and ferroin solutions were determined by weight of dissolved chemical. (See Table I for reactant concentrations.) Five different mesh ranges of analytical grade cation exchange resin were used (Table II). Nafion 417 (Aldrich), 0.4-mm sheets of perfluorinated cation-exchange membrane, was also used.

The reaction vessel consisted of a water-jacketed Petri dish with a plate glass bottom 12.5 cm in diameter. Solutions were maintained at $25.0 \pm 0.2^\circ\text{C}$ by water circulating through the jacket from a constant temperature bath. A Plexiglas lid positioned on top of the dish prevented disturbances by air currents.

Most experiments were monitored by taking photographs (35-mm slides) at timed intervals. Measurements of wave position as a function of time were made from the projected images. Some experiments were monitored with a digital imaging system. An image from a Newvicon video camera (Model 67M, Dage-MTI Inc.) attached to a zoom microscope (Model SV-8, Zeiss) was processed into a 485×496 array of pixels, each digitized to 256 gray levels. The imaging system (Model CAT-1631, Digital Graphics Systems) allows image addition, subtraction, multiplication, and division and similar manipulations between images and constant pixel values. The zoom microscope allows imaging of areas approximately 1.5×2.0 mm to 2.55×3.00 cm. The temporal resolution is $1/30$ s, the U.S. video standard; however, the resolution for successive images is limited by the time required for data storage on hard disk, about 1.5 min for a full image. A video cassette recorder allows examination of successive images at 1.0-s intervals, although the image quality is slightly degraded. Thin layers of ferroin-loaded cation-exchange resin were illuminated from below by light from a tungsten source passing through a 10-nm band-pass filter (centered at 440 nm).

Procedure. The cation-exchange resin was loaded with ferroin by mixing a measured quantity of beads with a measured volume of ferroin stock solution and stirring for 1.0 h. The ferroin solution typically became colorless within a few minutes. The smallest resin beads (diameter 38–75 μm), which were used in most of the experiments, were readily suspended in the reactant solution by gentle agitation. On settling, the 200.0-mL suspension containing 5.0 g of loaded beads formed a uniform thin film of resin on the bottom of the thermostated Petri dish. The thickness of the layer of beads, calculated from the volume of resin and the Petri dish surface area, was about 0.5 mm.

Wave velocity and wavelength were measured as a function of bromate concentration by preparing a series of reaction mixtures with all other concentrations held constant. Resin mesh size and quantity of ferroin-loaded resin per volume of reactant solution were also kept constant. In other experiments, the number of

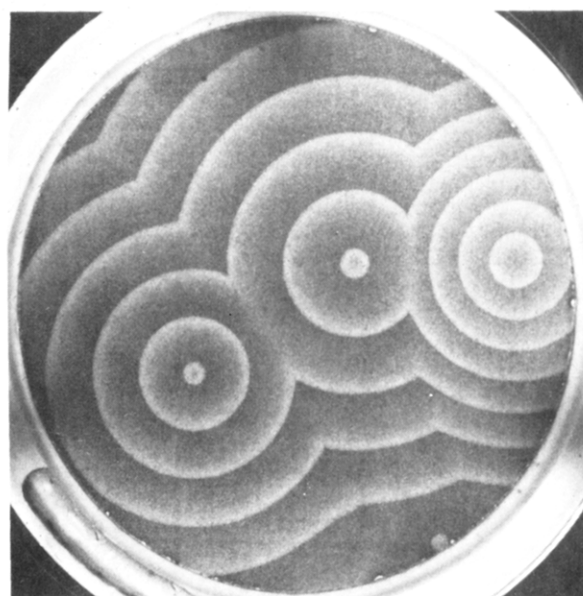


Figure 1. Chemical waves moving through thin film of ferroin-loaded cation-exchange resin covered with 1.6-cm layer of reactant solution. Composition in Table I with $[\text{BrO}_3^-] = 0.25$ M; resin size 1 in Table II. Photograph taken 85.0 min after the reagents were mixed. Petri dish diameter 12.5 cm.

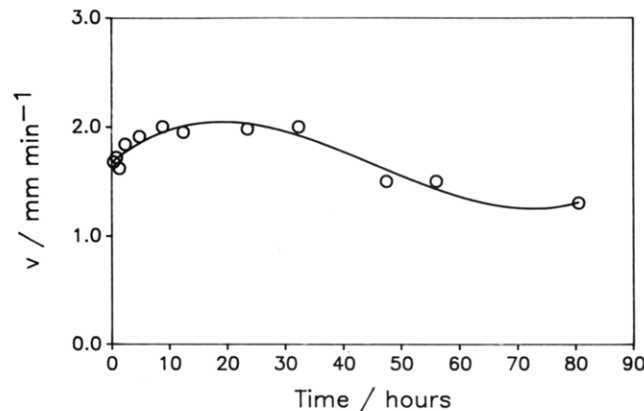


Figure 2. Wave propagation velocity over a period of 80.5 h. Composition in Table I with $[\text{BrO}_3^-] = 0.19$ M; resin size 1 in Table II.

spontaneous initiation sites was determined as a function of bromate concentration. The effects of resin mesh size were examined by loading the same amount of ferroin per gram of resin and mixing the loaded resin with 200.0 mL of reaction mixture of constant composition.

Nafion cation-exchange membrane was loaded with ferroin by immersing a section of membrane into a solution containing a large excess of ferroin. The red ferroin color of the membrane appeared to reach a maximum intensity after several days at which time it was assumed to be loaded to capacity.

Results

Duration of Pattern Formation. One of the most striking features of the Belousov-Zhabotinsky reaction with the ferroin catalyst immobilized on cation-exchange resin is the duration of the pattern formation. Shown in Figure 1 are typical target patterns in a system with relatively low bromate concentration and the smallest resin mesh size in Table II. The view is from above the Petri dish, looking through the colorless layer of reaction mixture to the thin layer of ferroin-loaded resin. For the particular resin bead size and reactant concentrations of this experiment, the propagating waves form uniform target patterns much like those exhibited in thin films of initially homogeneous BZ reaction mixtures.^{4,5,16–20} A major difference, however, is that target

(10) Rovinsky, A. B. *J. Phys. Chem.* **1987**, *91*, 4606.

(11) Vastano, J. A.; Pearson, J. E.; Horsthemke, W.; Swinney, H. L. *J. Chem. Phys.* **1988**, *88*, 6175.

(12) Kuramoto, Y. *Suppl. Prog. Theor. Phys.* **1978**, *64*, 346.

(13) Rovinsky, A. B. *J. Phys. Chem.* **1987**, *91*, 5113.

(14) Noszticzius, Z.; Horsthemke, W.; McCormick, W. D.; Swinney, H. L. *Nature* **1987**, *329*, 619.

(15) Tam, W. Y.; Horsthemke, W.; Noszticzius, Z.; Swinney, H. L. *J. Chem. Phys.* **1988**, *88*, 3395.

(16) Zhabotinsky, A. M.; Zaikin, A. N. *J. Theor. Biol.* **1973**, *40*, 45.

patterns in the classical BZ system typically occur for a few hours, while patterns like those in Figure 1 may be exhibited for days. Pattern formation for over 100 h was common and occasionally waves were exhibited for as long as 200 h. The duration of the pattern formation is dependent on reactant concentrations, with low bromate and sulfuric acid concentrations giving rise to longer lived patterns.

Shown in Figure 2 is the wave propagation velocity over a period of 80.5 h. Plots of wave position as a function of time over periods of 5–10 min were highly linear with least-squares correlation coefficients typically better than 0.99. The velocity calculated from these plots shows some drift (Figure 2); however, the variation is remarkably small considering the extended period of the experiment.

While wave velocity is relatively constant over long periods of time, the target patterns are continually changing, with new patterns of shorter wavelength replacing their predecessors. This phenomenon also occurs in the classical BZ system;⁵ however, the variation in wavelength is less pronounced than in the very long experiments reported here. Velocities in Figure 2 were measured from waves in four different target patterns, with wavelengths ranging from over 3.0 cm early in the experiment to less than 2.5 mm toward the end of the experiment. Target patterns of shorter and shorter wavelength give rise to an apparent lower limit in wavelength over extended experiments.

Studies of wave velocity in the classical BZ system have shown it to be dependent mainly on the concentrations of bromate and sulfuric acid, with less dependence on the concentrations of ferroin and malonic acid.^{4,5,17,19,21} We did not carry out a detailed study of velocity dependence on reactant concentrations; however, the dependence on initial bromate concentration was examined. Wave position as a function of time was measured in five experiments with all reactant concentrations held constant except that of BrO_3^- which was varied over the range in Table I. Velocities obtained from these measurements were plotted as a function of $[\text{BrO}_3^-]^{1/2}$, yielding the straight line (least-squares correlation coefficient 0.999) given by eq 1. Although the concentration of H_2SO_4 was

$$v/\text{mm min}^{-1} = -1.56 + 15.1[\text{H}_2\text{SO}_4]^{1/2}[\text{BrO}_3^-]^{1/2}/\text{M} \quad (1)$$

held constant (Table I), it is included in eq 1 to allow comparison with other studies of the velocity dependence. The slope of the straight line defined by eq 1 is about half that found in studies of the classical^{17,19,21} and modified BZ systems.^{22,23} The intercept is within the range of the previously reported values. Velocities given by eq 1 are typically less than half the velocities predicted for the classical system¹⁷ with the same BrO_3^- and H_2SO_4 concentrations.

The nearly constant velocity in Figure 2 indicates that reactant concentrations change little during the course of an experiment. The duration of the pattern formation appears to be related more to the decomposition of the ferroin catalyst than to the consumption of major reactants. The intensity of the color due to ferroin and ferriin gradually fades over time and eventually there is insufficient catalyst on the resin beads to support reaction.

Experiments were carried out to investigate the distribution of ferroin between the cation-exchange resin and aqueous solutions of the same acidity as in the experiments (Table I). With the smallest beads (size 1, Table II) loaded the same as in the wave experiments, a ferroin concentration of 5.2×10^{-7} M was measured by UV-vis spectrophotometry (molar absorption coefficient $1.11 \times 10^4 \text{ M}^{-1} \text{ cm}^{-1}$ at 510 nm)²⁴ in the 200.0-mL aqueous phase after mixing for 2.0 h. The distribution coefficient, defined as the concentration of ferroin on the resin (mol/g) divided by the

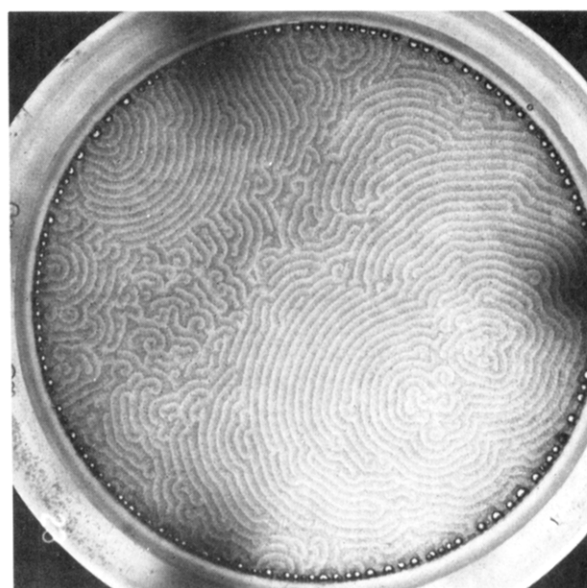


Figure 3. Target patterns with kinks and broken wave centers in thin film of ferroin-loaded cation-exchange resin covered with 1.6-cm layer of reactant solution. Also shown are regions of irregular patterns. Composition in Table I with $[\text{BrO}_3^-] = 0.50 \text{ M}$; resin size 4 in Table II. Photograph taken 24.0 h after the reagents were mixed. Petri dish diameter 12.5 cm.

concentration in solution (mol/g), for this level of loading is about 2×10^4 . Only when the resin was loaded to capacity (over 200 times the value in Table I) was ferroin in the aqueous phase detectable in significant quantities and then it corresponded to a loss from the resin of less than 0.1%. The extremely strong binding of ferroin to cation-exchange resin is apparently due to interaction of the 1,10-phenanthroline ligands with the polystyrene matrix of the resin. A similar interaction has been proposed to explain the strong binding of $\text{Ru}(\text{bpy})_3^{3+}$ in Nafion cation-exchange membrane.²⁵

The slow fading of color of the loaded resin beads is due to the ligand dissociation reactions of the $\text{Fe}(\text{phen})_3^{2+}$ and $\text{Fe}(\text{phen})_3^{3+}$ complexes. The dissociation of these complexes in H_2SO_4 solutions has been studied by Basolo and co-workers.²⁶ For the Fe(II) complex, $k_{\text{diss}} = 4.18 \times 10^{-3} \text{ min}^{-1}$ in 0.402 M H_2SO_4 and for the Fe(III) complex, $k_{\text{diss}} = 2.09 \times 10^{-3} \text{ min}^{-1}$ in 0.443 M H_2SO_4 . These rate constants predict essentially complete reaction (10 half-lives) of the Fe(II) complex in 27.6 h and the Fe(III) complex in 55.3 h at these H_2SO_4 concentrations. The dissociation constants for both complexes significantly decrease at higher concentrations of H_2SO_4 , apparently due to ion pairing with HSO_4^- .²⁶ We carried out semiquantitative experiments to check these results, periodically monitoring the optical absorbance (510 nm) of ferroin solutions with a range of H_2SO_4 concentrations. These measurements showed that the concentration of ferroin in solutions with high H_2SO_4 concentrations (e.g., 2.5 M) decreased more slowly than in solutions with lower H_2SO_4 concentrations (e.g., 0.1 M), in accord with the reported trend.²⁶ The high effective concentration of the sulfonic acid group within the cation-exchange resin along with the hydrophobic environment may explain the significantly slower dissociation rate of the complexes when bound to the resin. A general trend seemingly in conflict with the above results is the more rapid decomposition of the complexes in BZ reaction mixtures with high sulfuric acid concentrations. Apparently, the higher radical concentrations of these solutions provides a different pathway for the decomposition of ferroin and ferriin.

Qualitative Behavior. The pattern formation was photographically recorded at timed intervals for various concentrations

(17) Field, R. J.; Noyes, R. M. *J. Am. Chem. Soc.* **1974**, *96*, 2001.
(18) Showalter, K.; Noyes, R. M.; Turner, H. *J. Am. Chem. Soc.* **1979**, *101*, 7463.

(19) Wood, P. M.; Ross, J. *J. Chem. Phys.* **1985**, *82*, 1924.
(20) Ross, J.; Müller, S. C.; Vidal, C. *Science* **1988**, *240*, 460.
(21) Sevcikova, H.; Marek, M. *Physica D* **1983**, *9*, 140.
(22) Showalter, K. *J. Phys. Chem.* **1981**, *85*, 440.
(23) Kuhnert, L.; Krug, H.-J. *J. Phys. Chem.* **1987**, *91*, 730.
(24) Ford-Smith, M. H.; Sutin, N. *J. Am. Chem. Soc.* **1961**, *83*, 1830.

(25) Schmidt, M. H.; Lewis, N. S. *J. Phys. Chem.* **1988**, *92*, 2018.

(26) Dickens, J. E.; Basolo, F.; Neumann, H. M. *J. Am. Chem. Soc.* **1957**, *79*, 1286.

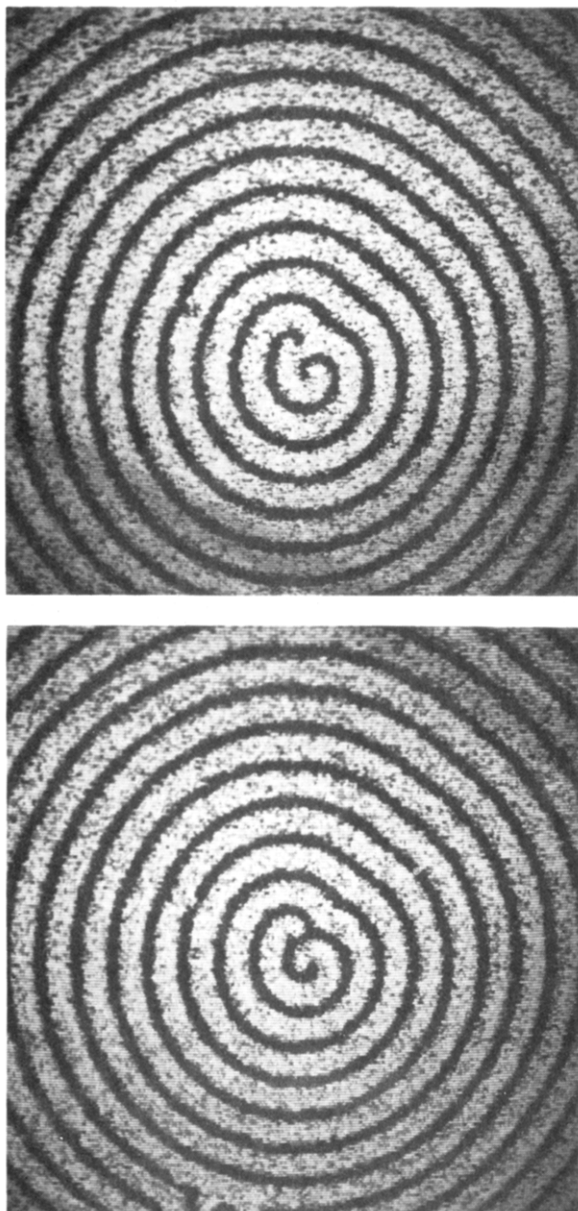


Figure 4. Difference images of target pattern with broken spiral center 131.7 min (above) and 132.0 min (below) after mixing reactants. Each image shows intensity (440 nm) difference between two images collected with a delay of 10.0 s. Dark bands represent distance that wave fronts have moved. Composition in Table I with $[BrO_3^-] = 0.3$ M; resin size 1 in Table II. Field of view 1.93×1.93 cm.

of BrO_3^- and resin mesh sizes. Irregularities appeared in the target patterns on increasing BrO_3^- concentration, and at high concentrations completely irregular patterns were exhibited. Similar behavior was found when the concentration of H_2SO_4 was increased; however, no detailed studies were carried out varying this reactant. The gradual transition to irregular behavior occurred at lower concentrations of BrO_3^- with larger bead sizes. Shown in Figure 3 is an example of mixed behavior with regions of fairly regular patterns interspersed with regions of irregular patterns. Even in the more regular regions, unusual kinks occur and the convoluted target patterns emanate from a core of broken waves. Resin size 4 (Table II) was used for Figure 3; similar behavior is exhibited with resin size 1 but at higher BrO_3^- concentration. The lower BrO_3^- concentration in Figure 3 resulted in a less oxidized medium (more red ferroin color), giving better contrast for the photograph.

The first sign of irregular behavior on increasing BrO_3^- concentration was the appearance of a broken wave segment at the center of some of the target patterns. Shown in Figure 4 are digitized images of this type of pattern. These images were

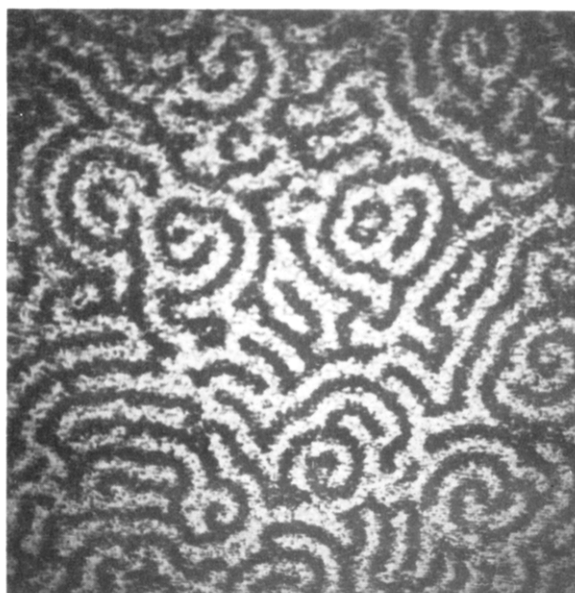


Figure 5. Difference image of irregular patterns 188.2 min after the reactants were mixed. Delay between subtracted images 20.0 s. Composition in Table I with $[BrO_3^-] = 0.45$ M; resin size 1 in Table II. Field of view 1.93×1.93 cm.

generated by subtracting an image giving light intensity at 440 nm from a similar image captured 10 s earlier. Pixels with negative values in the difference image are set to zero and appear as black. Thus, the dark bands represent the distance the wave front moved during the delay period between the primary images. This difference technique for examining wave fronts was necessary because of the heterogeneous nature of the system. The top image in Figure 4 shows a target pattern with counterrotating spirals at the center which serve to initiate the slightly distorted circular waves. A video tape of the pattern demonstrates that the unsymmetrical central wave segment rotates counterclockwise. The leading end behaves like a classical spiral wave and, as the wave segment rotates, the trailing end connects to form a closed circular wave, shown in the bottom image of Figure 4. The interior spiral wave is pinched off to form a new crescent, which undergoes another rotation to give birth to another wave of the target pattern. This behavior is characteristic of counterrotating spirals with centers of rotation too close for regular spiral waves to develop. Similar patterns can be generated in the homogeneous BZ system by mechanically shearing a wave into short segments. Counterrotating spirals in the classical system, however, are typically symmetrical with no leading and trailing ends as in Figure 4. The unsymmetrical character apparently arises during the spontaneous initiation process, considered below in the Discussion section.

Regions of irregular patterns appear as BrO_3^- concentration is increased to higher levels. The general appearance of these patterns is like that of the irregular regions in Figure 3. A difference image of irregular patterns in a system with resin bead size 1 is shown in Figure 5. The pattern is a collection of broken waves, some with a leading end like the central wave segment in Figure 4 and others without any apparent spiral character. Some of the segments develop into partial spirals, but kinks and twists occur throughout the pattern.

The temporal behavior of patterns like those in Figures 4 and 5 was examined by monitoring light intensity in a small area as a function of time. Shown in Figure 6 are plots of average light intensity (440 nm) as a function of time over an area of 0.015 mm^2 , representing a 5×5 grid of pixels in a magnified image. Figure 6a shows the periodic behavior of a target pattern with a broken wave center in a reaction mixture identical to that in Figure 4. Regular oscillations are exhibited with an average period of 57 ± 2 s. Figure 6b shows the periodic behavior of an irregular pattern in a reaction mixture identical with that in Figure 5. Regular oscillations are again found with an average period of 33 ± 2 s. Other sampling points in the irregular pattern showed

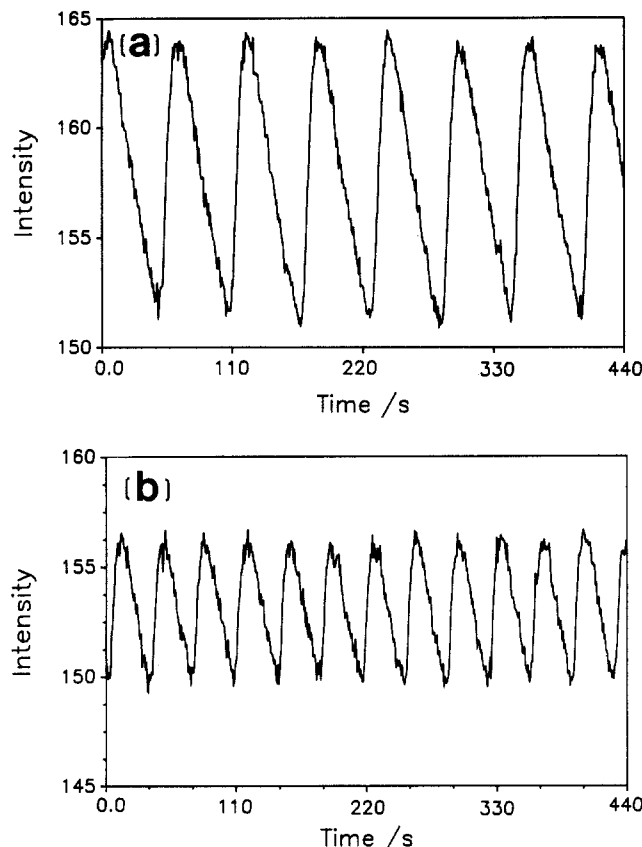


Figure 6. Intensity (gray level) as a function of time for target pattern (a) and irregular pattern (b). Composition and resin size same as in Figures 4 and 5 for (a) and (b), respectively. Intensity obtained by averaging gray level of pixels in magnified image, representing area of 0.015 mm^2 .

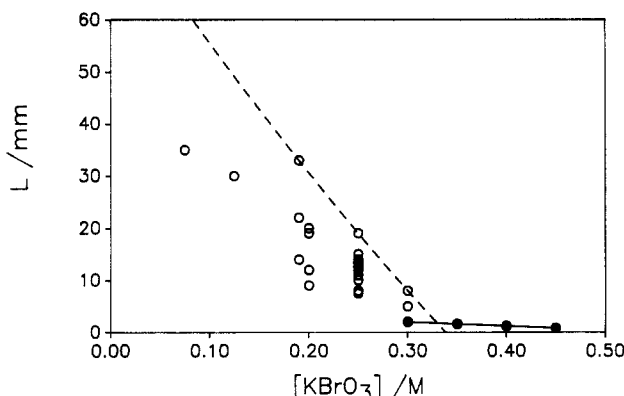


Figure 7. Wavelength L/mm as a function of BrO_3^- concentration. Dashed line shows approximate boundary of regular target patterns. Solid line shows wavelength of target patterns with counterrotating spirals as centers. Concentration of other reactants in Table I; resin size 1 in Table II.

simple oscillations like those in Figure 6b with essentially the same period. The noise in both oscillatory traces, but especially in Figure 6b, results from the low contrast of the patterns, giving a relatively small range of gray levels. The technique of averaging a number of adjacent pixels in a magnified image was designed to reduce the noise level in these measurements.

Concentration Dependence. Measurements of wavelength as a function of BrO_3^- concentration provide insight into the transition from regular to irregular behavior. Shown by the dashed line in Figure 7 is the approximate boundary of regular target patterns like those in Figure 1. Like the behavior seen in the classical BZ system,^{4,5} a variety of wavelengths are exhibited, indicated by the open circles. The wavelengths of target patterns with broken wave centers are shown by the solid circles. Because these patterns have a single wavelength at any particular BrO_3^- concentration, they

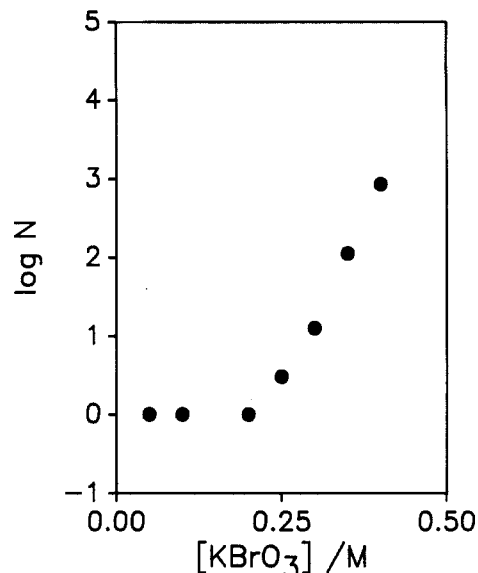


Figure 8. Number of initiation sites N 2.0 min after first appearance of wave initiation as a function of $[\text{BrO}_3^-]$. Concentrations of other reactants in Table I; resin size 1 in Table II. Petri dish diameter 12.5 cm.

define a line in the constraint-response diagram. At BrO_3^- concentrations above that defining the limit of regular target patterns, irregular patterns begin to appear. The wavelength of these patterns is difficult to determine because the behavior is not periodic in any given direction; however, the wave spacing seems to be equal to or less than that defined by the solid line in Figure 7.

In addition to wavelength and wave velocity dependence on BrO_3^- concentration, the effects of concentration on spontaneous wave initiation was studied. Figure 8 shows a plot of the number of initiation sites N as a function of BrO_3^- concentration. The value of N was determined by counting the sites 2.0 min after the first appearance of a spontaneous initiation. At BrO_3^- concentrations greater than about 0.3 M, a large number of initiation sites was exhibited and therefore only the sites in a small area were counted, with the value of N computed from the total area (122.7 cm^2). Figure 8 shows that at a BrO_3^- concentration of 0.4 M, waves were initiated at about 1000 sites in the Petri dish. Figure 7 shows that at BrO_3^- concentrations above about 0.34 M the initiations result in broken wave centers.

Discussion

The Belousov-Zhabotinsky reaction with ferroin immobilized on beads of cation-exchange resin offers a convenient experimental system for study of an inhomogeneous excitable medium. The characteristics due to the discrete nature of the medium can be examined by varying resin mesh size or reactant concentrations. The smallest beads form a uniform layer of resin that exhibits a transition from regular to irregular behavior on increasing the concentration of BrO_3^- . Larger beads exhibit behavior that is qualitatively the same, but at lower BrO_3^- concentrations. These beads, however, are less satisfactory for the formation of a uniform layer of resin.

In analyzing the chemical wave behavior of this system it is important to consider the characteristics of cation-exchange resin. In commercial electrolysis processes, cation-exchange membranes are used to prevent mixing of the anionic species in one cell with those of the other cell while allowing the transfer of cationic species. Anions do not significantly penetrate cation-exchange resin because the anionic portion of the sulfonic acid groups is covalently bound to the polystyrene matrix of the resin. Chemical reaction in the immobilized-catalyst BZ system is confined to the surface of the resin beads since the BrO_3^- anion is an essential reactant. The propagation velocity given by eq 1 is consistent with this feature. Velocities predicted by this equation are typically lower than the velocities measured by Field and Noyes¹⁷ in the classical BZ system. Assuming that the waves must propagate

around spherical beads rather than along a direct path suggests that the apparent linear velocity is lower than the actual velocity by a factor of $2/\pi$ or 0.64. (This factor is given by the direct path through a bead, $2r$, divided by one-half the circumference of the bead, πr , where r is the bead radius.) The actual velocity would be given by eq 2, which is just eq 1 multiplied by $\pi/2$, with $v' = (\pi/2)v$. Wave velocities measured by Field and Noyes¹⁷ in the

$$v'/\text{mm min}^{-1} = -2.45 + 23.7[\text{H}_2\text{SO}_4]^{1/2}[\text{BrO}_3]^{1/2}/\text{M} \quad (2)$$

homogeneous BZ system are described by eq 3. That velocities

$$v_{FN}/\text{mm min}^{-1} = -0.832 + 27.87[\text{H}^+]^{1/2}[\text{BrO}_3]^{1/2}/\text{M} \quad (3)$$

given by eq 2 are still somewhat lower than the values predicted by eq 3 may be due to delayed wave propagation between the beads. It seems unlikely that curvature effects²⁷ are of major importance for a wave propagating through the layer of beads because the effects of positive and negative curvature should tend to cancel.

Another important characteristic of cation-exchange resin is that it carries a net negative charge, resulting from the dissociation equilibrium of the fixed sulfonic acid groups. The negative charge gives rise to a double layer, which in an acidic medium contains an excess of hydrogen ions. In addition, the acidic beads used in our experiments have a very high effective concentration of hydrogen ion within the resin matrix and on the bead surface. It is the elevated hydrogen ion concentration from these sources that causes the beads to become initiation sites. As discussed below, however, the bead size plays a critical role in determining which beads become initiation sites.

The transition from regular to irregular spatial patterns is governed by two different but related features of the spatiotemporal behavior. One is the increase in wave initiation sites with increased activity of the system due to higher concentrations of BrO_3^- . This behavior, illustrated in Figure 8, is in accord with that of the homogeneous BZ system.^{4,5} The dependence of wave initiation on BrO_3^- and H_2SO_4 concentrations has been studied in the classical system by electrochemically depleting Br^- at a silver electrode.¹⁸ As either BrO_3^- or H_2SO_4 concentration was increased, the perturbation necessary to initiate a wave decreased, defined by the period of electrochemical consumption of Br^- at the electrode.

The increase in spontaneous initiation sites with increasing BrO_3^- concentration shown in Figure 8 is in qualitative agreement with Keener and Tyson's^{27,28} proposal that the initiation of a wave at a heterogeneous site can occur only if the radius of the particle exceeds some critical value. Their analysis predicts a critical radius given by $2D/v$, where D is the diffusion coefficient of the autocatalyst and v is the propagation velocity. More initiation sites occur with an increase in BrO_3^- concentration because the critical radius for excitation varies inversely with the square root of BrO_3^- and H_2SO_4 concentrations. The number of initiation sites with resin size 1 increases sharply at a BrO_3^- concentration of about 0.25 M, as shown in Figure 8. We expect the critical radius to correspond to that of the largest beads in resin size 1, about 0.038 mm, when the beads begin to serve as initiation sites. The velocity given by eq 3 for the homogenous system¹⁷ at this BrO_3^- concentration predicts a critical radius of 0.039 mm, assuming a value for D of $2.0 \times 10^{-3} \text{ mm}^2 \text{ s}^{-1}$, in good agreement with the expected critical radius. As BrO_3^- concentration is increased, the critical radius decreases, and a larger fraction of the beads become initiation sites. The size distribution of beads within a particular mesh size is given by a fairly sharp peak centered at the average bead size with shallow tails extending to the limits of the mesh range, according to the manufacturer's specifications (Aldrich). The greatest number of initiation points in Figure 8 represents less than 0.01% of the total number of beads, suggesting that the large beads serving as initiation sites fall in the tail (high side) of the size distribution curve. Consistent with this picture is the observation that the number of initiation sites increases with

increasing resin mesh size for a particular BrO_3^- concentration.

Playing an equally important role in the transition from regular to irregular pattern formation is the spontaneous appearance of broken wave segments, which give rise to counterrotating spirals. Spontaneous formation of spirals is not observed in the classical BZ system. Spiral formation in the initially homogeneous reaction occurs when a propagating wave is mechanically sheared, either by mixing with a stirring rod or by gentle agitation of the solution.^{4,5} The spontaneous initiation of spirals in the immobilized-catalyst system is due to the inhomogeneous nature of the excitable medium. Excitation of adjacent beads to form an unsymmetrical initiation site is not adequate to explain the observed broken wave segments. The behavior of simple cellular automata^{29,30} shows that this type of initiation site would result only in an unsymmetrical target pattern. On the other hand, an excited cell adjacent to a cluster of cells unable to be excited can give rise to a broken wave segment.³¹ Holes resulting from packing defects in the layer of resin beads would be consistent with this model; however, it is unlikely that such defects would occur at every initiation site, which number in the hundreds at high BrO_3^- concentrations. More likely is that the different bead sizes give rise to "excitation defects". The resin bead diameters within a mesh size, shown in Table II, range over a factor of 2 for sizes 1 and 2, and vary over larger ranges for sizes 3–5. As suggested above, the high surface curvature of the small beads results in these beads being more difficult to excite. Easily excited large beads serve as initiation sites while adjacent clusters of less easily excited small beads serve as excitation defects. While these differing excitabilities play a critical role in the initiation process, wave propagation seems to be unaffected, apparently because all beads become excited by the steep concentration gradient of bromous acid in the wave front. The excitation defects become unimportant at low BrO_3^- concentrations because the adjacent larger beads are also below the critical size and cannot serve as initiation sites. The few target patterns that appear, like those in Figure 1, are apparently initiated at anomalous sites, such as a few large beads outside the mesh size range. These initiation sites and resulting target patterns are centrosymmetric like those observed in the classical BZ reaction because the layer of resin beads is homogeneous in the sense that essentially all the beads are below the critical size for spontaneous wave initiation.

The transition from symmetrical to spiral initiation sites is a key element in the appearance of irregular patterns. The broken wave centers give rise to target patterns, all of a single wavelength dependent only on the system composition. When the number of initiations is such that there is no longer sufficient room for the formation of target patterns, irregular behavior occurs. A rough calculation based on the area required for the innermost circular wave of the target pattern in Figure 4 (top) shows that less than 500 of these waves would completely fill the Petri dish, assuming hexagonal packing. Figure 8 shows that at BrO_3^- concentrations between 0.35 and 0.4 M the number of initiation sites exceeds 500. Figure 7 shows that at BrO_3^- concentrations above 0.34 M all initiation sites become counterrotating spirals. In accord with these observations, irregular spatial patterns are exhibited at BrO_3^- concentrations above about 0.35 M. If only symmetrical initiation sites occurred, target patterns with a variety of wavelengths would develop and eventually the pattern with the shortest wavelength would fill the medium.^{4,5} Thus, the high density of initiation sites, all of which generate waves at the same frequency, gives rise to the irregular behavior.

The appearance of broken wave centers of target patterns is accompanied by the appearance of kinks in otherwise regular target patterns. As shown in Figure 3, a wave running parallel to another wave suddenly bends around to connect with the following wave. Similar kinks were observed in the experiments of Krinsky and Agladze³² in which low-frequency waves overtaken

(29) Wolfram, S. *Nature* 1984, 311, 419.

(30) Greenberg, J. M.; Hastings, S. P. *SIAM J. Appl. Math.* 1978, 34, 515.

(31) Maselko, J.; Showalter, K., unpublished results.

(32) Krinsky, V. I.; Agladze, K. I. *Physica D* 1983, 8, 50.

by waves from a high-frequency source resulted in multiarmed spirals. The kinks in the immobilized catalyst system are apparently the result of lower frequency symmetrical initiation sites being overtaken by higher frequency broken wave sites.

The irregular patterns exhibited by the immobilized-catalyst BZ reaction vaguely resemble the "mosaic" patterns reported in the homogeneous BZ system^{16,33,34} and modified BZ systems.^{35,36} These patterns, however, are different in character and origin. The patterns in the classical BZ system involve a hydrodynamic instability of the excitable reaction mixture. Convective flow in the immobilized-catalyst system plays the role of reactant and product transport to and from the site of reaction on the catalyst beads. The convective flow is probably influenced by the chemical waves which in turn might affect the waves and resulting pattern. However, our experiments show that the pattern formation is extremely robust provided that the layer of resin is not mechanically disrupted and it seems unlikely that the behavior is significantly affected by the convective flow.

A variety of configurations are possible in an immobilized-catalyst BZ reaction. Our study has focused on the characteristics of a nonuniform excitable medium. The smallest resin size in Table II is particularly well suited for such a study. The bead diameters range over a factor of 2 and the bead size is sufficiently small that an even layer of resin beads is easily made. Some bead size differentiation probably occurs on settling, giving rise to a vertical size gradient within the thin layer; however, the horizontal bead size distribution should be quite random.

Another attractive configuration of an immobilized-catalyst system would be an open system, continually supplied with fresh reactants. The resin bead system studied here is not suitable for such a configuration because the layer of resin is disrupted when the reactant solution is mechanically stirred. More suitable for an open system is one based on immobilizing the ferroin catalyst on cation-exchange membrane. A simple continuous-flow, stirred reactor with the membrane suspended in the solution would be easily configured. Unfortunately, cation-exchange membrane is usually quite nonuniform due to reinforcement fibers. The most uniform cation-exchange membrane we have found is Nafion 417, unreinforced 0.4-mm sheets of perfluorinated polymer with sulfonic acid sites. Our preliminary results with this material show that patterns of extremely short wavelength (0.2 mm) occur on ferroin-loaded membrane bathed in reactant solutions similar to those in Table I. However, gross variations in the wavelengths of the patterns occur, suggesting that either the membrane or the mass transport to and from the membrane is not uniform. Work is in progress to determine the source of these nonuniformities. A very uniform immobilized-catalyst surface might be prepared by covalently attaching the 1,10-phenanthroline ligand or another suitable ligand to commercially available derivatizable polystyrene or to glass by a silane linkage. It should be noted that reactant consumption is not a significant problem in the immobilized-ferroin

system reported here. However, an open system is attractive because the system constraints can be systematically varied, allowing examination of transitions from one behavior to another at bifurcation points.

Conclusion

Our study of the Belousov-Zhabotinsky reaction with the ferroin catalyst immobilized shows that a wealth of interesting spatial behavior occurs in this undeveloped, yet easily realized configuration. We believe that this and other immobilized-catalyst systems offer an important link to pattern formation in the inherently inhomogeneous systems common to biology and chemical engineering. The excitable media in biological systems such as heart muscle or nerve tissue are clearly inhomogeneous. Cell size differences and differences in membrane transport may give rise to characteristics similar to those seen in the system studied here. Pattern formation on inhomogeneous catalytic surfaces bathed in reactant gases is also closely related. Many chemical manufacturing processes are carried out over fixed-bed catalysts and it seems likely that product yield in these processes could be affected by chemical waves and associated pattern formation.

Theoretical studies of spatial chaos have focused on homogeneous systems with inhomogeneous initial conditions.^{12,13} Phase turbulence and amplitude turbulence have been proposed¹² as sources of spatial chaos in which the former results in chaotic spatial behavior and periodic temporal behavior while the latter results in both spatial and temporal chaos. Figures 5 and 6b show that, while the spatial behavior of the immobilized-catalyst system may be very irregular, the temporal behavior is quite periodic. Several features of the system studied here suggest that the irregular behavior is an example of phase turbulence. Although the irregular behavior depends on the inhomogeneity of the medium, it is during the wave initiation process that the inhomogeneity plays a critical role. Wave propagation is little affected by the inhomogeneity of the medium. Thus, to a degree, the system may be viewed as a homogeneous excitable medium with inhomogeneous initial conditions.

Our study shows that the spatial behavior of this immobilized-catalyst BZ system is governed by variations in excitability of the inhomogeneous medium. Spontaneous initiations of chemical waves give rise to irregular behavior when the initiation site density exceeds available space for uniform pattern formation. Equally important is that each spontaneous initiation above a critical BrO_3^- concentration generates a broken wave segment, resulting in counterrotating spirals. These features, a critical density of spontaneous initiations, each with spiral character, constitute the recipe for irregular spatial behavior in this inhomogeneous excitable medium.

Acknowledgment. This paper is dedicated with gratitude and admiration to Richard M. Noyes. K.S. thanks John J. Tyson for an informative discussion concerning the spatial behavior reported in this paper. This work was supported by the National Science Foundation (Grant No. CHE-8613240).

Registry No. BrO_3^- , 15541-45-4; malonic acid, 141-82-2; ferroin, 14708-99-7.

(33) Agladze, K. I.; Krinsky, V. I.; Petsov, A. M. *Nature* **1984**, *308*, 834.

(34) Müller, S. C.; Plessner, Th.; Hess, B. *Physica D* **1987**, *24*, 71.

(35) Showalter, K. *J. Chem. Phys.* **1980**, *73*, 3735.

(36) Orbán, M. *J. Am. Chem. Soc.* **1980**, *102*, 4311.